Patterning and Electronic Tuning of Laser Scribed Graphene for Flexible All-Carbon Devices

Veronica Strong,[†] Sergey Dubin,[†] Maher F. El-Kady,[†,⊥] Andrew Lech,[†] Yue Wang,[†] Bruce H. Weiller,[‡] and Richard B. Kaner[†,§,*]

[†]Department of Chemistry and Biochemistry and California NanoSystems Institute, University of California, Los Angeles, Los Angeles, California 90095, United States, [‡]Micro/Nano Technology Department, Space Materials Laboratory, The Aerospace Corporation, Los Angeles, California 90009, United States, [§]Department of Materials Science and Engineering, University of California, Los Angeles, Los Angeles, California 90095, United States, and [⊥]Department of Chemistry, Faculty of Science, Cairo University, Giza 12613, Egypt

ABSTRACT Engineering a low-cost graphene-based electronic device has proven difficult to accomplish *via* a single-step fabrication process. Here we introduce a facile, inexpensive, solid-state method for generating, patterning, and electronic tuning of graphene-based materials. Laser scribed graphene (LSG) is shown to be successfully produced and selectively patterned from the direct laser irradiation of graphite oxide films under ambient conditions. Circuits and complex designs are directly patterned onto various flexible substrates without masks, templates, post-processing, transferring techniques, or metal catalysts. In addition, by varying the laser intensity and laser irradiation treatments, the electrical properties of LSG can be precisely tuned over 5 orders of magnitude of conductivity, a feature that has proven difficult with other methods. This inexpensive method for generating LSG on thin flexible substrates provides a mode for fabricating a low-cost graphene-based NO_2 gas sensor and enables its use as a heterogeneous scaffold for the selective growth of Pt nanoparticles. The LSG also shows exceptional electrochemical activity that surpasses other carbon-based electrodes in electron charge transfer rate as demonstrated using a ferro-/ferricyanide redox couple.

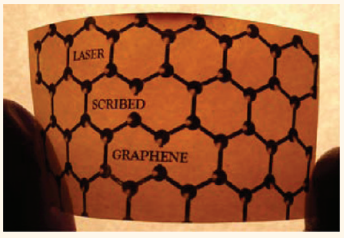

KEYWORDS: laser patterning · graphene · graphite oxide · flexible electronics · gas sensor · graphene/Pt composite · electrocatalysis

In the pursuit of producing high-quality bulk graphene-based devices, a variety of syntheses now incorporate graphite oxide (GO) as a precursor for the generation of large-scale graphene-based materials.[1] This inexpensive method of producing large quantities of GO from the oxidation of graphitic powders, in addition to its water dispersibility, has made GO an ideal starting material. In particular, the water dispersibility of GO, which stems from the electronegative oxygen species bonded to the carbon network,[2] has led, through exfoliation, to the production of individual graphene oxide sheets.[3] Unfortunately, the same oxygen species that give GO its water-dispersible properties also create defects in its electronic structure, and as a result, GO is an electrically insulating material.[4] Therefore, the development of device grade graphene-based films with superior electronic properties requires the removal of these oxygen species, re-establishment of the conjugated carbon network, as well as a method for controllably patterning electronic device features.[5]

Methods for reducing graphite oxide have included chemical reduction *via* hydrazine, hydrazine derivatives or other reducing agents,[6−8] high-temperature annealing under chemical reducing gases and/or inert atmospheres,[9] solvothermal reduction,[10,11] a combination of chemical and thermal reduction methods,[12] flash reduction,[13,14] and most recently, laser reduction of GO.[15−19] Although several of these methods have demonstrated relatively high-quality reduction of graphite oxide, many have been limited by expensive equipment, high annealing temperatures, and nitrogen impurities in the final product. In addition, large-scale film patterning *via* an all-encompassing step for both reduction and patterning has proven difficult and has typically been dependent on photomasks to provide the most basic of patterns. Therefore, an inexpensive process that does not need reducing agents and expensive equipment and is highly tunable is essential to produce high-quality graphene-based films at low cost. The technique described here not only meets these stringent requirements but also provides direct control over film conductivity and image patterning, creating flexible electronic devices in a single-step process.

* Address correspondence to kaner@chem.ucla.edu.

Received for review October 31, 2011 and accepted January 13, 2012.

Published online January 13, 2012
10.1021/nn204200w

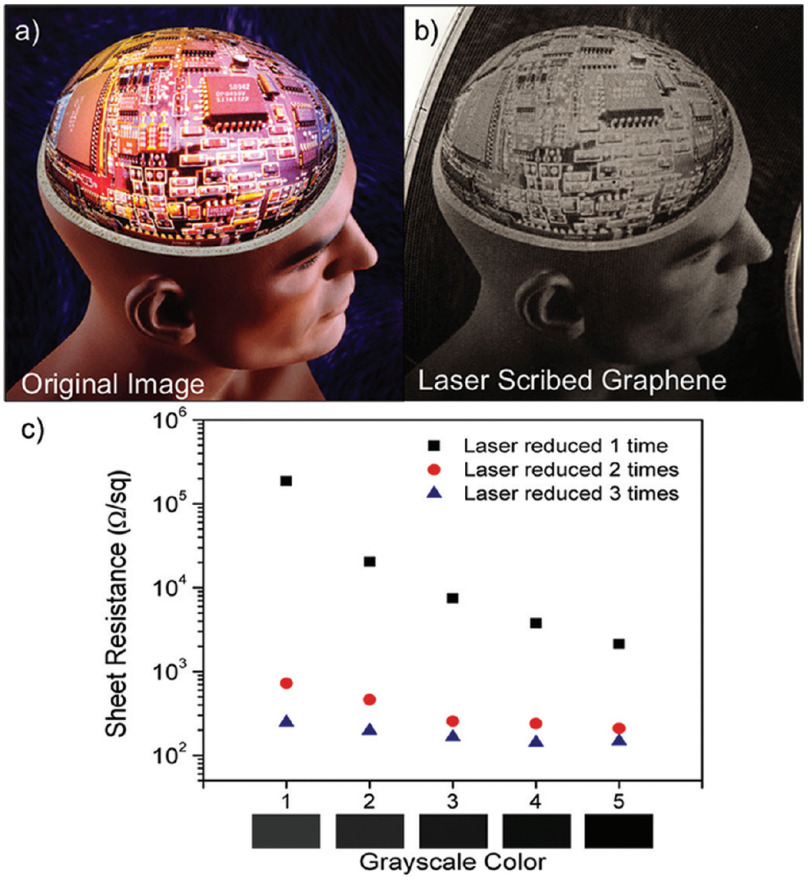

Figure 1. Comparison between (a) a standard complex colored image of a man's head filled with circuits and (b) the same image reproduced by reducing graphite oxide at various levels, which corresponds to a change in electrical properties (Copyright Lester Lefkowitz). A correlation between laser intensity and sheet resistance is shown in (c) where the sheet resistance of LSG is controlled in two ways, by printing in grayscale color and/or by controlling the number of times the film is irradiated with the 788 nm infrared laser. The log base graph clearly shows the sheet resistance decreasing by orders of magnitude when different grayscale colors are used, which is directly related to the laser intensity. In addition, the number of times the graphite oxide film is irradiated with that specific grayscale color, for example, laser reduced once (black squares), twice (red dots), or three time (blue triangles), also produces a significant decrease in sheet resistance, which provides a second mode of controlling the electrical properties of LSG.

The simple direct fabrication of laser scribed graphene (LSG) on flexible substrates therefore simplifies the development of lightweight electronic devices. Here, an all-organic NO_2 gas sensor, a fast redox-active electrode, and a scaffold for the direct growth of platinum nanoparticles are demonstrated.

RESULTS AND DISCUSSION

Here we show that LightScribe patterning technology can be used as an effective tool for solid-state patterning and generation of laser scribed graphene. LightScribe is a commercially available program that is used in conjunction with a DVD optical drive unit to pattern images on any LightScribe-enabled CD/DVD disk.[20] The program controls the 788 nm infrared laser (maximum power output = 5 mW) inside an optical drive unit by periodically pulsing an objective lens assembly, causing the laser to focus and defocus on an infrared active dye matrix found on the top side of a LightScribe-enabled CD/DVD disk. In order to control the objective lens pulsing mechanism and hence the laser intensity, the LightScribe program uses a computerized grayscale to generate different levels of contrast in the resulting pattern. Thus by focusing the laser on a specific area of the dye matrix, it is possible to selectively pattern complex images[20] (see Supporting Information). Here we bypass the original dye matrix by depositing a thin layer of graphite oxide on top of a DVD disk prior to the patterning process and use the LightScribe program to effectively and controllably reduce and pattern graphite oxide films.

As an illustration of the diversity in image patterning that is possible, a complex image formed by the direct laser reduction of graphite oxide is shown in Figure 1. An elaborate image of a man's head with circuits (Figure 1a) is directly patterned on a film of graphite oxide (Figure 1b). Essentially, any part of the graphite oxide film that comes in direct contact with the 788 nm infrared laser is effectively reduced, with the amount of reduction being controlled by the laser intensity, a

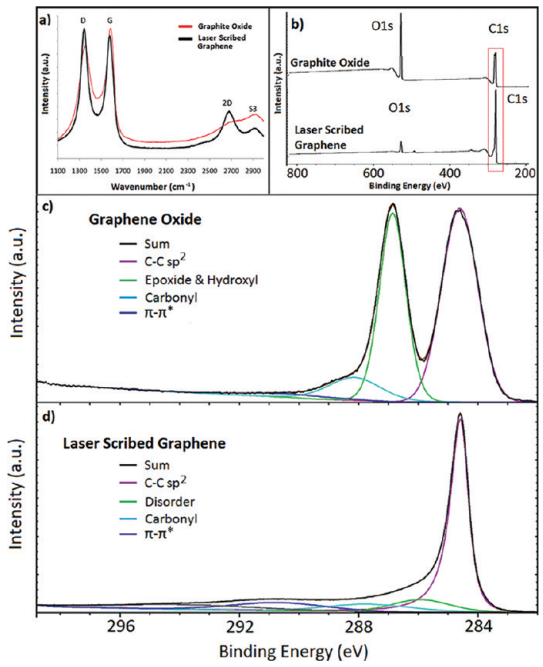

Figure 2. Raman and X-ray photoelectron spectroscopic (XPS) comparisons between GO and hr-LSG. (a) Raman showing graphite oxide (solid red line) exhibiting typical D, G, and amorphous 2D bands. The LSG (solid black line) spectrum shows an increase in the D band due to an increase in edge planes after laser irradiation as well as a shifted and diminished G band as a result of the enhanced crystallinity of the LSG. The shift and presence of the 2D band indicates the synthesis of few-layer graphene. (b) Overview of the XPS spectra confirms the decrease in the ratio of oxygen to carbon as a result of laser irradiation of the graphite oxide film. By taking a closer look at the boxed area, it is possible to compare the carbon−oxygen functionalities of (c) graphite oxide and (d) laser scribed graphene. In contrast to graphite oxide, the LSG film shows a significant loss of C−O functionalities, an increase in sp^2 carbons, and a significant increase in the π to π^* satellite peak.

factor that is determined by the degree of laser focus and/or pulsing of the objective lens assembly unit. The resulting image is an effective print of the original image, but it is set in a series of gray and black colors, which is directly related to the laser intensities that are used to generate the image. As expected, the darkest black areas indicate exposure to the strongest laser intensities, while the lighter gray areas are only partially reduced. Since different grayscale colors directly correlate with the laser's intensity, it is possible to tune the electrical properties of the generated LSG over 5 orders of magnitude in sheet resistance (Ω/sq) by simply changing the grayscale color used during the patterning process. In fact, there is a clear relationship between sheet resistance, grayscale color, and the number of times the graphite oxide film is laser irradiated, as illustrated in Figure 1c. Control over conductivity from a completely insulating graphite oxide film, with typical sheet resistance values of >20 MΩ/sq to a conducting highly reduced laser scribed graphene (hr-LSG) registering a sheet resistance value of approximately 80 Ω/sq, which translates to a conductivity of ∼1650 S/m, is possible. This method is sensitive enough to differentiate between visibly similar grayscale colors, as shown in the graph, with the sheet resistance varying significantly with only a small change in grayscale. In addition, the number of times a film is laser-treated results in a significant and controllable change in sheet resistance. Each additional laser treatment lowers the sheet resistance, as seen in Figure 1c, where a film is laser-reduced once (black squares), twice (red circles), and three times (blue triangles) with respect to the grayscale. Therefore, the film's sheet resistance is tunable by controlling both the grayscale color used and the number of times the film is reduced by the laser, a property that has so far been difficult to control through other methods.

Raman spectroscopy was used to characterize and compare the structural changes induced by laser treating graphite oxide. As can be seen in Figure 2a, characteristic D, G, 2D, and 3S peaks are observed in both graphite oxide and highly reduced laser scribed graphene. The presence of the D band in both spectra suggests that carbon sp^3 centers still exist after reduction.[6] The LSG spectrum shows a slight increase in the D band peak at ∼1350 cm^{-1}; this unexpected increase is due to a larger presence of structural edge defects and indicates an overall increase in the amount of smaller graphene domains.[21] The result is consistent with SEM analysis, where the generation of exfoliated accordion-like graphitic regions (Supporting Information Figure S2) caused by the laser treatment creates a large amount of edges.[22,23] However, the D band also shows a significant overall peak narrowing, suggesting a decrease in the types of defects in the laser scribed graphene. The G band experiences a narrowing and a decrease in peak intensity as well as a peak shift from 1585 to 1579 cm^{-1}. These results are consistent with the re-establishment of sp^2 carbons and a decrease in structural defects within the basal planes.[24,25] The overall changes in the G band indicate a transition from an amorphous carbon state to a more crystalline carbon state. In addition, a prominent and shifted 2D peak from 2730 to 2688 cm^{-1} is seen after GO is treated with the infrared laser, indicating a considerable reduction of the GO film and strongly points to the presence of few layer graphene (see Supporting Information).[26,27] Finally, as a result of lattice disorder, the combination of D−G generates an S3 second-order peak, which appears at ∼2927 cm^{-1} and, as expected, diminishes with decreasing disorder after infrared laser treatment.[28] The Raman analysis demonstrates the effectiveness of treating graphite oxide with an infrared laser as a means to effectively and controllably produce few-layer laser scribed graphene.

X-ray photoelectron spectroscopy (XPS) was employed to correlate the effects of laser irradiation on the oxygen functionalities and to monitor the

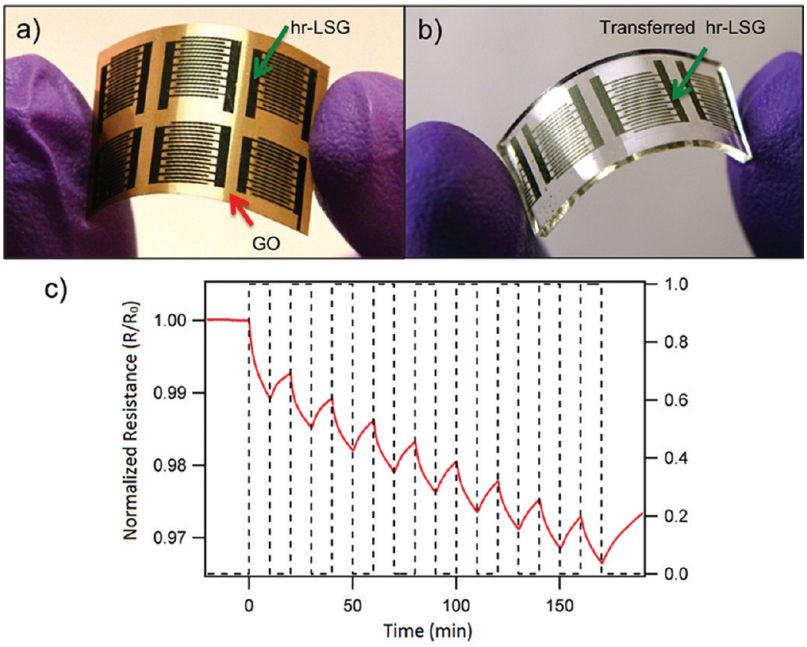

Figure 3. (a) All-organic flexible set of interdigitiated electrodes generated from highly reduced laser scribed graphene (hr-LSG). (b) Same interdigitated electrodes transferred onto polydimethylsiloxane (PDMS). (c) NO_2 detection using the same all-organic flexible interdigitated electrodes. Here the sensor uses hr-LSG as the active electrodes and marginally laser-reduced graphite oxide as the detecting media. The NO_2 concentration is 20 ppm in dry air gas.

structural changes in the GO film. Comparing the carbon to oxygen (C/O) ratios between graphite oxide and highly reduced laser scribed graphene provides an effective measurement of the extent of reduction achieved using a simple low-energy infrared laser. Figure 2b illustrates the significant disparity between the C/O ratios before and after laser treatment of the graphite oxide films. Prior to laser reduction, typical graphite oxide films have a C/O ratio of approximately 2.6, corresponding to a carbon/oxygen content of ~72 and 38%. On the other hand, the hr-LSG has an enhanced carbon content of 96.5% and a diminished oxygen content of 3.5%, giving an overall C/O ratio of 27.8. Since the laser reduction process takes place under ambient conditions, it is postulated that some of the oxygen present in the hr-LSG film is a result of the film having a static interaction with oxygen found in the environment.

The C1s XPS spectrum of GO displays two broad peaks (Figure 2c), which can be resolved into three different carbon components corresponding to the functional groups typically found on the GO surface, in addition to a small π to π^* peak at 290.4 eV.[21] These functional groups include carboxyl, sp^3 carbons in the form of epoxide, and hydroxyl carbons, which are associated with the following binding energies: approximately 288.1, 286.8, and 284.6 eV, respectively.[29,30] As expected, the large degree of oxidation in graphite oxide results in the various oxygen components in the GO C1s XPS spectrum, in contrast to the highly reduced laser scribed graphene spectrum, which shows a significant decrease in oxygen-containing functional groups and an overall increase in the C−C sp^2 carbon peak (Figure 2d). This points to an efficient deoxygenation process as well as the re-establishment of C═C bonds in the carbon network. These results are consistent with the Raman analysis. Thus the infrared laser is powerful enough to remove a majority of the oxygen functional groups, as is evident in the LSG XPS spectrum, which only shows a small disorder peak and a peak at 287.6 eV. The latter corresponds to the presence of sp^3-type carbons, suggesting that a small amount of carboxyl groups remain in the final product. In addition, the presence of a π to π^* satellite peak at ~290.7 eV is found, indicating that delocalized π conjugation is significantly stronger in the highly reduced laser scribed graphene as this peak is miniscule in the graphite oxide XPS spectrum.[31] The appearance of the delocalized π peak is a clear indication that conjugation in the GO film is restored during the laser reduction process and adds support that an sp^2 carbon network has been re-established. The decreased intensity of the oxygen-containing functional groups, the dominating C−C bond peak, and the presence of the delocalized π conjugation all indicate that a low-energy infrared laser is an effective tool in the generation of hr-LSG.

Having established that hr-LSG has effective π conjugation, it is possible to construct devices to make use of the conducting material. Figure 3a shows a set of interdigitated electrodes with dimensions of 6 mm × 6 mm, spaced at ~500 μm, that are directly patterned onto a thin film of graphite oxide. Prior to being patterned, the graphite oxide film was deposited on

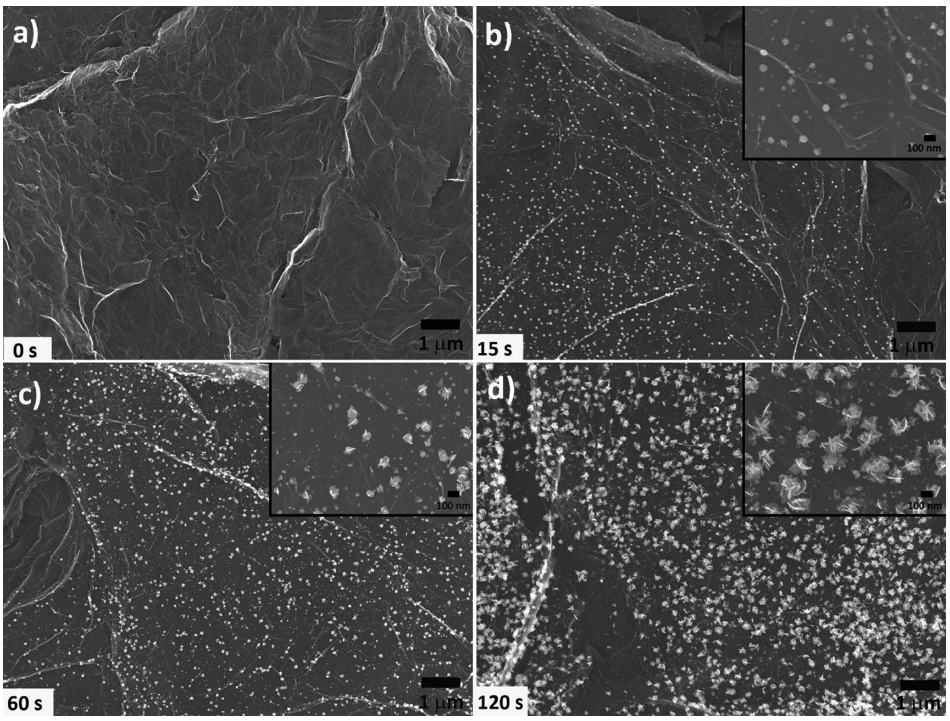

Figure 4. Scanning electron microscopy (SEM) analysis of platinum nanoparticle growth on LSG films. LSG is shown to be an excellent heterogeneous scaffold for the growth of platinum nanoparticles by electrochemically reducing 1 mM K_2PtCl_4 + 0.5 M H_2SO_4 at −0.25 V for (a) 0 s, (b) 15 s, (c) 60 s, and (d) 120 s. The result is an increase in the size of the Pt nanoparticles as a function of electrodeposition time. The insets in b−d show a magnified view of each set of nanoparticles, with nanoparticles ranging from 10 to 50 nm after 15 s to 200−300 nm after 120 s. Inset scale bars = 100 nm.

a thin flexible substrate, polyethylene terephthalate (PET), in order to fabricate a set of electrodes that are mechanically flexible. A green arrow points to the laser scribed graphene region that makes up the black interdigitated electrodes, while a red arrow points to the unreduced golden colored graphite oxide film. Since the electrodes are directly patterned onto the GO film on a flexible substrate, the necessity for post-processing, such as transferring the film to a new substrate, is unnecessary. Although, if desired, a peel and stick method could be used to selectively lift-off the LSG with, for example, polydimethylsiloxane (PDMS) and transfer it onto other types of substrates (Figure 3b). The simplicity of this method allows substantial control over pattern dimensions, substrate selectivity, and even the electrical properties of the LSG by controlling the laser intensity and thereby the amount of reduction in each film.

These interdigitated electrodes can in turn be used as an all-organic flexible gas sensor for the detection of NO_2. Figure 3c shows the sensor response for a patterned flexible set of interdigitated LSG electrodes that are exposed to 20 ppm of NO_2 in dry air. This sensor was fabricated by patterning hr-LSG as the active electrode and marginally reducing the area between the electrodes to have a consistent sheet resistance of ∼7775 Ω/sq. In this way, it is possible to bypass the use of metal electrodes and directly pattern both the electrode and the sensing material on the flexible substrate simultaneously. The plot relates NO_2 gas exposure to R/R_0, where R_0 is the sheet resistance at the initial state and R is the resistance of the LSG film after exposure to the gas. The film was exposed to NO_2 gas for 10 min followed immediately by purging with air for another 10 min. This process was then repeated nine more times for a total of 200 min. Even with a slightly lower sensitivity than more sophisticated and optimized sensors, the unoptimized LSG sensor still shows good, reversible sensing for NO_2, and its easy fabrication makes it quite advantageous for these systems.[32,33] Therefore, the LSG sensor for NO_2 holds promise for improving the fabrication of all-organic flexible sensor devices at low cost by using inexpensive starting materials directly patterned with an inexpensive laser.

The high conductivity and the increase in surface area resulting from the expanded LSG make this material a viable candidate for use as a heterogeneous catalyst for metal nanoparticles. In particular, the direct growth of platinum nanoparticles on LSG could aid in the improvement of methanol-based fuel cells, which have shown enhanced device performance from large surface area and conducting carbon-based scaffolds.[34] Here, we demonstrate that hr-LSG is a viable scaffold for the controllable growth of Pt nanoparticles. By electrochemically reducing 1 mM of K_2PtCl_4 with 0.5 M H_2SO_4 at −0.25 V for different periods of time, it is possible to actively control the platinum particle

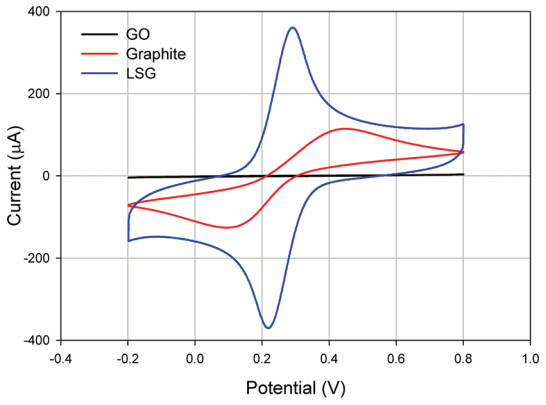

Figure 5. CV profiles of graphite oxide (GO), graphite, and hr-LSG electrodes in equimolar mixture (5 mM) of $K_3[Fe(CN)_6]/K_4[Fe(CN)_6]$ dissolved in 1.0 M KCl solution at a scan rate of 50 mV/s. The hr-LSG electrode approaches the behavior of a perfect reversible system with a peak-to-peak potential of 59.5 mV at 10 mV/s, which is close to the theoretical Nerstian value of 59 mV. The hr-LSG shows high electron transfer rates, 105 times faster than graphite and even higher than values reported for carbon nanotube electrodes[43,44] and stacked graphene nanofibers.[45]

size that is electrodeposited on the hr-LSG film. Figure 4 shows scanning electron microscopy images illustrating the growth of Pt nanoparticles with respect to electrodeposition times corresponding to 0, 15, 60, and 120 s. As expected, there are no platinum particles present at 0 s of electrodeposition (Figure 4a), but small Pt nanoparticles are clearly visible after just 15 s (Figure 4b) with nanoparticle sizes ranging from 10 to 50 nm (Figure 4b, inset). After 60 s of electrodeposition, larger platinum nanoparticles grow with particle sizes averaging 100 to 150 nm (Figure 4c). Finally, after 120 s, 200 to 300 nm particles are found evenly distributed across the surface of the LSG. The active growth of Pt nanoparticles at controllable diameters on LSG could make it a potentially useful hybrid material for applications that require metal nanoparticles, such as methanol fuel cells and gas phase catalysts.[35−38] These applications are now being explored.

Carbon electrodes have attracted tremendous interest for various electrochemical applications because of their wide potential window and good electrocatalytic activity for many redox reactions.[39,40] Given its high surface area and flexibility and the fact that it is an all-carbon electrode, laser scribed graphene could revolutionize electrochemical systems by making miniaturized and fully flexible devices. Here, understanding the electrochemical properties of laser scribed graphene is highly beneficial to determine its potential for electrochemical applications. Recently, graphene's electrocatalytic properties have been demonstrated to stem, in large part, from the efficient electron transfer at its edges rather than its basal planes. In fact, it has been reported that graphene exhibits in certain systems electrocatalytic activity similar to that of edge plane highly ordered pyrolytic graphite.[41] In addition to having a highly expanded network, hr-LSG also displays a large amount of edge planes (see Supporting Information, Figure S2), making it an ideal system for studying the role of edge planes on the electrochemistry of graphene-based nanomaterials. Here, we explore the electrochemical behavior associated with the electron transfer of flexible hr-LSG electrodes using an $[Fe(CN)_6]^{3-/4-}$ couple as a redox probe. Figure 5 compares the CV profiles of GO, graphite, and hr-LSG electrodes in an equimolar mixture of 5 mM $K_3[Fe(CN)_6]/K_4[Fe(CN)_6]$ dissolved in 1.0 M KCl solution at a scan rate of 50 mV/s. Unlike GO and graphite, the hr-LSG electrode approaches the behavior of a perfectly reversible system with a low ΔE_p (peak-to-peak potential separation) of 59.5 mV at a scan rate of 10 mV/s to 97.6 mV at a scan rate 400 mV/s. The low ΔE_p values approach the calculated theoretical value of 59 mV. Given that ΔE_p is directly related to the electron transfer rate constant (k^0_{obs}), the low experimental value of ΔE_p indicates a very fast electron transfer rate.[42] The calculated k^0_{obs} values vary from 1.266×10^{-4} cm s^{-1} for graphite and as expected increases for hr-LSG to 1.333×10^{-2} cm s^{-1} (see Experimental Section and Supporting Information for calculations). In addition to the impressive increase in the electron transfer rate at the hr-LSG electrode (2 orders of magnitude faster than a graphite electrode), there is also substantial electrochemical activity for the hr-LSG electrode as seen by an increase of ~268% in the voltammetric peak current. These drastic improvements are attributed to the expanded architecture of hr-LSG films, which provide large open areas for the effective diffusion of the electroactive species and allow a better interfacial interaction with the LSG surface. Additionally, it is surmised that the amount of edge-like surface per unit mass is thus much higher than graphite and therefore contributes to the higher electron transfer rates as seen here. Given the large number of exposed edge sites in hr-LSG, it is not surprising to find that it not only has a higher k^0_{obs} value than graphite but also surpasses that of carbon-nanotube-based electrodes[43,44] and that of stacked graphene nanofibers.[45]

Note that the hr-LSG electrodes are fabricated on flexible PET substrates covered with graphite oxide, which when laser-reduced serves as both the electrode and the current collector, thus making this particular electrode not only lightweight and flexible but also inexpensive. In addition, the low oxygen content in hr-LSG (~3.5%), as shown through XPS analysis, is quite advantageous to the electrochemical activity seen here since a higher oxygen content at the edge plane sites has been shown to limit and slow down the electron transfer of the ferri-/ferrocyanide redox couple.[46] We believe this new process presents an interesting methodology for making highly electroactive electrodes for potential applications in vapor sensing, biosensing, electrocatalysis, and energy storage.

CONCLUSION

A new method has been presented for producing graphene-based materials that is not only facile, inexpensive, and versatile but is a one-step "green" process for reducing and patterning graphene films in the solid state. A simple low-energy, inexpensive infrared laser is used as a powerful tool for the effective reduction and subsequent expansion and exfoliation and fine patterning of graphite oxide. Aside from the ability to directly pattern and effectively produce large areas of highly reduced laser scribed graphene films, this method is applicable to a variety of other thin substrates and has the potential to simplify the manufacturing process of devices made entirely from organic materials. A flexible all-organic gas sensor has been fabricated directly by laser patterning of graphite oxide deposited on thin flexible PET. LSG is also shown to be an effective scaffold for the successful growth and size control of Pt nanoparticles *via* a simple electrochemical process. Finally, a flexible hr-LSG electrode was fabricated, which displays a textbook-like reversibility with an impressive increase of ~238% in electrochemical activity when compared to graphite toward the electron transfer between the ferri-/ferrocyanide redox couple. This proof-of-concept process has the potential to effectively improve applications that would benefit from the high electrochemical activity demonstrated here including batteries, sensors, and electrocatalyts.

EXPERIMENTAL SECTION

Graphene oxide was synthesized using a modified Hummers method,[47] with dispersions of graphene oxide prepared according to the following concentrations: 3.7, 2.8, and 1.6 mg/mL. Approximately, 16 mL of the respective graphite oxide solutions was drop-casted directly onto a LightScribe-enabled CD/DVD media disk and allowed to dry for 24 h. Spin-coating was also a technique that was used to make films of GO, but depending on the substrate used and the type of experiment needed, drop-casting was typically the better choice for this work. In order to increase the hydrophilicity of the substrate surface and obtain thin uniform films, the LightScribe-enabled DVD substrates were pretreated with an oxygen plasma at 35 mW for 3 min. A thick film of polydimethylsiloxane (PDMS) was used to cover and protect the tracking strip found at the center of the DVD disk from the oxygen plasma. The graphite oxide dispersion was also drop-cast onto a thin substrate such as polyethylene terephthalate (PET), which was resized to the same dimension as the DVD and affixed onto the CD/DVD surface for laser treatment. Silver electrodes with dimensions of 1 mm × 3 mm with an interelectrode spacing of 3 mm were deposited on the laser-reduced and non-laser-treated graphite oxide films and subsequently divided into pairs. Two-point $I-V$ measurements were carried out using a standard probe station. Ten or more measurements were performed on different areas of each film to ensure reproducibility. The film thicknesses were measured on a Dektak 6 profilometer. Sheet resistance and conductivity values were calculated from two-point probe measurements and the film thicknesses.

The LSG morphology was monitored and imaged using an optical microscope (Zeiss Axiotech 100) and a scanning electron microscope (JEOL 6700, Philips XL 30). XPS spectra were recorded using a Kratos Axis Ultra DLD spectrometer. A Renishaw RAMAN spectrometer with an excitation wavelength of 514 nm was employed to characterize the structural changes between graphite oxide and laser scribed graphene. Sensor experiments were carried out as described by Fowler *et al.*[32]

Electrochemical Experiments. All electrochemical experiments were performed with an electrochemical analyzer VeraSTAT3 (Princeton Applied Research, USA). A three-electrode configuration was employed for all of the measurements with a platinum foil counter electrode (6.25 cm^2, Sigma-Aldrich) and a Ag/AgCl, 3 M NaCl reference electrode (Bioanalytical Systems Inc., USA). The working electrodes used were hr-LSG, graphite oxide, or graphite electrodes, all with a working surface area of 0.16 cm^2.

Each hr-LSG electrode was made by cutting a PET sheet coated with hr-LSG into rectangular pieces of the appropriate size. The ends were then lightly painted with conducting silver paint to ensure good electrical contact. Part of the electrode was then covered with polyimide (Kapton) tape so that only a working area of 0.16 cm^2 was allowed to be exposed to the electrolyte. Finally, the electrode was connected to the potentiostat with an alligator clip. Each graphite oxide electrode was prepared by a similar approach using graphite oxide coated PET. Pencil lead obtained from Pentel Co. Ltd., Japan, and named Hi-polymer Super 50-HB was purchased from a local store and used as a graphite electrode. The "lead" had a total length of 6 cm and a diameter of 0.07 cm. The electrode was prepared by renewing its surface using cellophane tape before its use. This procedure involves pressing the surface onto a cellophane tape and removing the top few layers of graphite. After repeating several times, the electrode was then cleaned in acetone to remove any adhesive. A projected surface of 0.16 cm^2 was obtained by sealing part of the electrode with Kapton tape.

Electron Transfer Kinetics. The redox system that was used for the evaluation of the electron transfer kinetics was 5 mM $K_3[Fe(CN)_6]/K_4[Fe(CN)_6]$ (1:1 molar ratio) dissolved in 1.0 M KCl solution. To ensure a stable electrochemical response, the electrodes were first cycled for at least five scans before collecting the experimental data. The heterogeneous electron transfer rate constant (k^0_{obs}) was determined using a method developed by Nicholson, which relates the peak separation (ΔE_p) to a dimensionless kinetic parameter, ψ, and consequently to k^0_{obs} according to the following equation:[48]

$$k^0_{obs} = \psi\left[\sqrt{D_0 \pi \nu \left(\frac{nF}{RT}\right)}\right]\left(\frac{D_R}{D_O}\right)^{\alpha/2} \quad (1)$$

where D_O and D_R are the diffusion coefficients of the oxidized and reduced species, respectively. The other variables include ν, the applied scan rate; n, the number of electrons transferred in the reaction; F, the Faraday constant; R, the gas constant; T, the absolute temperature; and α, the transfer coefficient. The diffusion coefficients of the oxidized and reduced species are typically similar; therefore, the term $(D_R/D_O)^{\alpha/2} \sim 1$. A diffusion coefficient (D_O) of 7.26×10^{-6} cm^2 s^{-1} was used for $[Fe(CN)_6]^{3-/4-}$ in 1.0 M KCl.[49]

Synthesis of Platinum Nanoparticles/hr-LSG Composites. Electrodeposition of Pt nanoparticles on hr-LSG electrodes was performed in a three-electrode cell (described above) containing 1.0 mM K_2PtCl_6 in 0.5 M H_2SO_4 at a constant potential of −0.25 V. To control the amount and size of the Pt nanoparticles, the deposition was carried out for different periods of time.

Conflict of Interest: The authors declare no competing financial interest.

Acknowledgment. S.D. and M.F.E.-K. contributed equally to this work. We thank J. Fowler for obtaining preliminary sensor data, K. Cha and J. Wassei for Raman experiments, and J. D'Arcy for helpful discussions. NSF-Graduate Research Fellowship (Y.W.). The UCLA Nanoelectronics Research Facility provided access to a clean room with a Dektak Stylus Surface Profiler. Support for this research comes from the UCLA-based Focused Center Research Program in Functional Engineered NanoArchitectonics Center (R.B.K.), the Mitsubishi Chemical Center for Advanced Materials (R.B.K.), and The Aerospace Corporation's Independent Research and Development Program (B.H.W.).

Supporting Information Available: Characterization information with corresponding figures and discussion, including UV–vis, powder XRD, SEM, TEM, and electron transfer kinetics. This material is available free of charge *via* the Internet at http://pubs.acs.org.

REFERENCES AND NOTES

1. Compton, O. C.; Nguyen, S. T. Graphene Oxide, Highly Reduced Graphene Oxide, and Graphene: Versatile Building Blocks for Carbon-Based Materials. *Small* **2010**, *6*, 711–723.
2. Zhu, Y.; Stoller, M. D.; Cai, W.; Velamakanni, A.; Piner, R. D.; Chen, D.; Ruoff, R. S. Exfoliation of Graphite Oxide in Propylene Carbonate and Thermal Reduction of the Resulting Graphene Oxide Platelets. *ACS Nano* **2010**, *4*, 1227–1233.
3. De, S.; King, P. J.; Lotya, M.; O'Neill, A.; Doherty, E. M.; Hernandez, Y.; Duesberg, G. S.; Coleman, J. N. Flexible, Transparent, Conducting Films of Randomly Stacked Graphene from Surfactant-Stabilized, Oxide-Free Graphene Dispersions. *Small* **2010**, *6*, 458–464.
4. Jung, I.; Dikin, D. A.; Piner, R. D.; Ruoff, R. S. Tunable Electrical Conductivity of Individual Graphene Oxide Sheets Reduced at "Low" Temperatures. *Nano Lett.* **2008**, *8*, 4283–4287.
5. Stankovich, S.; Piner, R. D.; Chen, X.; Wu, N.; Nguyen, S. T.; Ruoff, R. S. Stable Aqueous Dispersions of Graphitic Nanoplatelets *via* the Reduction of Exfoliated Graphite Oxide in the Presence of Poly(sodium-4-styrenesulfonate). *J. Mater. Chem.* **2006**, *16*, 155–158.
6. Stankovich, S.; Dikin, D. A.; Piner, R. D.; Kohlhaas, K. A.; Kleinhammes, A.; Jian, Y.; Wu, Y.; Nguyen, S. T.; Ruoff, R. S. Synthesis of Graphene-Based Nanosheets *via* Chemical Reduction of Exfoliated Graphite Oxide. *Carbon* **2007**, *45*, 1558–1565.
7. Gilje, S.; Han, S.; Wang, M.; Wang, K. L.; Kaner, R. B. A Chemical Route to Graphene for Device Applications. *Nano Lett.* **2007**, *7*, 3394–3398.
8. Tung, V. C.; Allen, M. J.; Yang, Y.; Kaner, R. B. High-Throughput Solution Processing of Large-Scale Graphene. *Nat. Nanotechnol.* **2009**, *4*, 25–29.
9. McAllister, M. J.; Li, J.-L.; Adamson, D. H.; Schniepp, H. C.; Abdala, A. A.; Liu, J.; Herrera-Alonso, M.; Milius, D. L.; Car, R.; Prud'homme, R. K.; *et al.* Single Sheet Functionalized Graphene by Oxidation and Thermal Expansion of Graphite. *Chem. Mater.* **2007**, *19*, 4396–4404.
10. Dubin, S.; Gilje, S.; Wang, K.; Tung, V. C.; Cha, K.; Hall, A. S.; Farrar, J.; Varshneya, R.; Yang, Y.; Kaner, R. B. A One-Step, Solvothermal Reduction Method for Producing Reduced Graphene Oxide Dispersions in Organic Solvents. *ACS Nano* **2010**, *4*, 3845–3852.
11. Wang, H.; Robinson, J. T.; Li, X.; Dai, H. Solvothermal Reduction of Chemically Exfoliated Graphene Sheets. *J. Am. Chem. Soc.* **2009**, *131*, 9910–9911.
12. Eda, G.; Fanchini, G.; Chhowalla, M. Large-Area Ultrathin Films of Reduced Graphene Oxide as a Transparent and Flexible Electronic Material. *Nat. Nanotechnol.* **2008**, *3*, 270–274.
13. Gilje, S.; Dubin, S.; Badakhshan, A.; Farrar, J.; Danczyk, S. A.; Kaner, R. B. Photothermal Deoxygenation of Graphene Oxide for Patterning and Distributed Ignition Applications. *Adv. Mater.* **2010**, *22*, 419–423.
14. Cote, L. J.; Cruz-Silva, R.; Huang, J. Flash Reduction and Patterning of Graphite Oxide and Its Polymer Composite. *J. Am. Chem. Soc.* **2009**, *131*, 11027–11032.
15. Abdelsayed, V.; Moussa, S.; Hassan, H. M.; Aluri, H. S.; Collision, M. M.; El-Shall, M. S. Photothermal Deoxygenation of Graphite Oxide with Laser Excitation in Solution and Graphene-Aided Increase in Water Temperature. *J. Phys. Chem. Lett.* **2010**, *1*, 2804–2809.
16. Huang, L.; Liu, Y.; Ji, L.-C.; Xie, Y.-Q.; Wang, T.; Shi, W.-Z. Pulsed Laser Assisted Reduction of Graphene Oxide. *Carbon* **2011**, *49*, 2431–2436.
17. Sokolov, D. A.; Shepperd, K. R.; Orlando, T. M. Formation of Graphene Features from Direct Laser-Induced Reduction of Graphite Oxide. *J. Phys. Chem. Lett.* **2010**, *1*, 2633–2636.
18. Zhang, Y.; Guo, L.; Wei, S.; He, Y.; Xia, H.; Chen, Q.; Sun, H.-B.; Xiao, F.-S. Direct Imprinting of Microcircuits on Graphene Oxides Film by Femtosecond Laser Reduction. *Nano Today* **2010**, *5*, 15–20.
19. Gao, W.; Singh, N.; Song, L.; Liu, Z.; Reddy, A. L. M.; Ci, L.; Vajtai, R.; Zhang, Q.; Wei, B.; Ajayan, P. M. Direct Laser Writing of Micro-Supercapacitors on Hydrated Graphite Oxide Films. *Nat. Nanotechnol.* **2011**, *6*, 496–500.
20. Stinson, D. G.; Maguire, M. *LightScribe Direct Disc Labeling*, **2005**.
21. Yang, D.; Velamakanni, A.; Bozoklu, G.; Park, S.; Stoller, M. D.; Piner, R. D.; Stankovich, S.; Jung, I.; Field, D. A.; Ventrice, C. A., Jr.; *et al.* Chemical Analysis of Graphene Oxide Films After Heat and Chemical Treatments by X-ray Photoelectron and Micro-Raman Spectroscopy. *Carbon* **2009**, *47*, 145–152.
22. Ferrari, A. C.; Meyer, J. C.; Scardaci, V.; Casiraghi, C.; Lazzeri, M.; Mauri, F.; Piscanec, S.; Jiang, D.; Novoselov, K. S.; Roth, S. Raman Spectrum of Graphene and Graphene Layers. *Phys. Rev. Lett.* **2006**, *97*, 187401–187404.
23. Cong, C. X.; Yu, T.; Ni, Z. H.; Liu, L.; Shen, Z. X.; Huang, W. Fabrication of Graphene Nanodisk Arrays Using Nanosphere Lithography. *J. Phys. Chem. C* **2009**, *113*, 6529–6532.
24. Tuinstra, F.; Koenig, J. L. Raman Spectrum of Graphite. *J. Chem. Phys.* **1970**, *53*, 1126–1130.
25. Kudin, K. N.; Ozbas, B.; Schniepp, H. C.; Prud'homme, R. K.; Aksay, I. A.; Car, R. Raman Spectra of Graphite Oxide and Functionalized Graphene Sheets. *Nano Lett.* **2008**, *8*, 36–41.
26. Ferrari, A. C. Raman Spectroscopy of Graphene and Graphite: Disorder, Electron–Phonon Coupling, Doping and Nonadiabatic Effects. *Solid State Commun.* **2007**, *143*, 47–57.
27. Dato, A.; Radmilovic, V.; Lee, Z.; Phillips, J.; Frenklach, M. Substrate-Free Gas-Phase Synthesis of Graphene Sheets. *Nano Lett.* **2008**, *8*, 2012–2016.
28. Cuong, T. V.; Pham, V. H.; Tran, Q. T.; Hahn, S. H.; Chung, J. S.; Shin, E. W.; Kim, W. J. Photoluminescence and Raman Studies of Graphene Thin Films Prepared by Reduction of Graphene Oxide. *Mater. Lett.* **2010**, *64*, 399–401.
29. Dreyer, D. R.; Park, S.; Bielawski, C. W.; Ruoff, R. S. The Chemistry of Graphene Oxide. *Chem. Soc. Rev.* **2010**, *39*, 228–240.
30. Shin, H.-J.; Kim, K. K.; Benayard, A.; Yoon, S.-M.; Park, H. K.; Jung, I.-S.; Jin, M. H.; Jeong, H.-K.; Kim, J. M.; Choi, J.-Y. Efficient Reduction of Graphite Oxide by Sodium Borohydride and Its Effect on Electrical Conductance. *Adv. Funct. Mater.* **2009**, *19*, 1987–1992.
31. Gao, W.; Alemany, L. B.; Ci, L.; Ajayan, P. M. New Insights into the Structure and Reduction of Graphite Oxide. *Nat. Chem.* **2009**, *1*, 403–408.
32. Fowler, J. D.; Allen, M. J.; Tung, V. C.; Yang, Y.; Kaner, R. B.; Weiller, B. H. Practical Chemical Sensors from Chemically Derived Graphene. *ACS Nano* **2009**, *3*, 301–306.
33. Robinson, J. T.; Perkins, F. K.; Snow, E. S.; Wei, Z.; Sheehan, P. E. Reduced Graphene Oxide Molecular Sensors. *Nano Lett.* **2008**, *8*, 3137–3140.
34. Li, Y.; Gao, W.; Ci, L.; Wang, C.; Ajayan, P. M. Catalytic Performance of Pt Nanoparticles on Reduced Graphene

Oxide for Methanol Electro-Oxidation. *Carbon* **2010**, *48*, 1124–1130.
35. Qiu, J.-D.; Wang, G.-C.; Liang, R.-P.; Xia, X.-H.; Yu, H. W. Controllable Deposition of Platinum Nanoparticles on Graphene as an Electrocatalyst for Direct Methanol Fuel Cells. *J. Phys. Chem. C* **2011**, *115*, 15639–15645.
36. Seger, B.; Kamat, P. V. Electrocatalytically Active Graphene–Platinum Nanocomposites. Role of 2-D Carbon Support in PEM Fuel Cells. *J. Phys. Chem. C* **2009**, *113*, 7990–7995.
37. Ha, H.-W.; Kim, I. Y.; Hwang, S.-J.; Ruoff, R. S. One-Pot Synthesis of Platinum Nanoparticles Embedded on Reduced Graphene Oxide for Oxygen Reduction in Methanol Fuel Cells. *Electrochem. Solid State* **2011**, *14*, B70–B73.
38. Moussa, S.; Abdelsayed, V.; El-Shall, M. S. Laser Synthesis of Pt, Pd, CoO and Pd–CoO Nanoparticle Catalysts Supported on Graphene. *Chem. Phys. Lett.* **2011**, *510*, 179–184.
39. Chen, D.; Tang, L.; Li, J. Graphene-Based Materials in Electrochemistry. *Chem. Soc. Rev.* **2010**, *39*, 3157–3180.
40. Yang, W.; Ratinac, K. R.; Ringer, S. P.; Thordarson, P.; Gooding, J. J.; Braet, F. Carbon Nanomaterials in Biosensors: Should You Use Nanotubes or Graphene? *Angew. Chem., Int. Ed.* **2010**, *49*, 2114–2138.
41. Kampouris, D. K.; Banks, C. E. Exploring the Physicoelectrochemical Properties of Graphene. *Chem. Commun.* **2010**, *46*, 8986–8988.
42. Hallam, P. M.; Banks, C. E. Quantifying the Electron Transfer Sites of Graphene. *Electrochem. Commun.* **2011**, *13*, 8–11.
43. Pumera, M.; Sasaki, T.; Iwai, H. Relationship between Carbon Nanotube Structure and Electrochemical Behavior: Heterogeneous Electron Transfer at Electrochemically Activated Carbon Nanotubes. *Chem. Asian J.* **2008**, *3*, 2046–2055.
44. Streeter, I.; Wildgoose, G. G.; Shao, L.; Compton, R. G. Cyclic Voltammetry on Electrode Surfaces Covered with Porous Layers: An Analysis of Electron Transfer Kinetics at Single-Walled Carbon Nanotube Modified Electrodes. *Sens. Actuators, B* **2008**, *133*, 462–466.
45. Ambrosi, A.; Bonanni, A.; Pumera, M. Electrochemistry of Folded Graphene Edges. *Nanoscale* **2011**, *3*, 2256–2260.
46. Ji, X.; Banks, C. E.; Crossley, A.; Compton, R. G. Oxygenated Edge Plane Sites Slow the Electron Transfer of the Ferro-/Ferricyanide Redox Couple at Graphite Electrodes. *ChemPhysChem* **2006**, *7*, 1337–1344.
47. Kovtyukhova, N. I.; Oliver, P. I.; Martin, B. R.; Mallouk, T. E.; Chizhik, S. A.; Buzaneva, E. V.; Gorchinskiy, A. D. Layer-by-Layer Assembly of Ultrathin Composite Films from Micron-Sized Graphite Oxide Sheets and Polycations. *Chem. Mater.* **1999**, *11*, 771–778.
48. Nicholson, R. S. Theory and Application of Cyclic Voltammetry for Measurement of Electrode Reaction Kinetics. *Anal. Chem.* **1965**, *37*, 1351–1355.
49. Konopka, S. J.; McDuffie, B. Diffusion Coefficients of Ferri- and Ferrocyanide Ions in Aqueous Media, Using Twin-Electrode Thin-Layer Electrochemistry. *Anal. Chem.* **1970**, *42*, 1741–1746.